Biomedicine & Pharmacotherapy xxx (xxxx) xxx–xxx

Contents lists available at ScienceDirect

Biomedicine & Pharmacotherapy

journal homepage: www.elsevier.com/locate/biopha

Activation of Epac alleviates inflammation and vascular leakage in LPS-induced acute murine lung injury

Xuefeng Wang[a,1], Shunde Song[b,1], Zhengqiang Hu[b,1], Zhewen Zhang[b], Yajun Li[b], Chunguang Yan[c], Zigang Li[d], Huifang Tang[b,*]

[a] Second Affiliated Hospital, Zhejiang Chinese Medical University, Hangzhou 310005, China
[b] Zhejiang Respiratory Drugs Research Laboratory, School of Basic Medical Sciences, Zhejiang University, Hangzhou, Zhejiang 310058, China
[c] Department of Pathogenic Biology and Immunology, Southeast University School of Medicine, Nanjing 210009, China
[d] Department of Anesthesiology, Women's Hospital, Zhejiang University, School of Medicine, Hangzhou 310006, China

ARTICLE INFO

Keywords:
LPS
Acute lung injury
cAMP
Epac
PKA

ABSTRACT

Exchange protein directly activated by cAMP (Epac) is an important molecule in cAMP signal transduction, but the effect of Epac on lipopolysaccharide (LPS)-induced acute lung injury (ALI) is unclear. In this study, we treated *in vitro* and *in vivo* models with the Epac activator 8CPT to determine the effect and related mechanisms of Epac. The *in vitro* results indicate that 8CPT inhibits lipopolysaccharide (LPS)-induced tumor necrosis factor-α (TNF-α) release from mouse macrophages (MH-S), whereas the protein kinase A (PKA) activator 6BnZ has no effect. Furthermore, Epac over-expression can significantly suppress TNF-α release from LPS induced MH-S cell, while Epac siRNA can slightly increase TNF-α release. Moreover, 8CPT reduces LPS-induced microvascular permeability in human pulmonary microvascular endothelial cells (HPMVECs), whereas the PKA activator 6BnZ has no effect. In mice with LPS-induced ALI, 8CPT significantly reduces LPS-induced inflammatory cytokine release, neutrophil recruitment, and albumin leakage. LPS simultaneously decreases the Epac but not the PKA levels. However, 8CPT reverses the decreased Epac levels. Furthermore, the mechanism involves the small GTPase Rac1/2 but not the mitogen-activated protein kinase (MAPK) pathway. Thus, Epac activation reduces inflammation and microvascular permeability in LPS-induced lung injury and an Epac activator represents a novel choice for the early therapy of ALI.

1. Introduction

High incidences of acute lung injury (ALI) and acute respiratory distress syndrome (ARDS) have been noted, but therapies are still lacking [1]. Lipopolysaccharide (LPS) is a major component of gram-negative bacteria and is widely used to induce and investigate the molecular mechanisms of acute inflammatory injury of the lung [2]. As shown in our previous studies, an intratracheal instillation of LPS activates alveolar macrophages, resulting in the production of early-response cytokines, such as tumor necrosis factor-α (TNF-α), interleukin-1β (IL-1β), and IL-6. LPS then induces a strong pro-inflammatory cascade that eventually causes acute damage to capillary and alveolar epithelial cells [3].

Clinical and basic studies have revealed beneficial effects of elevated intracellular cAMP levels in various pathological settings, such as pulmonary edema [4] and ischemia-reperfusion (I-R) injury in isolated blood-perfused rabbit lungs [5]. In previous studies of ALI, cAMP was shown to exert protective effects on various animal models, such as *Escherichia coli*-induced ALI in guinea pigs [6], protamine-induced ALI in isolated rat lungs [7], endotoxin-induced lung injury in rats [8], and pulmonary air embolism-induced lung injury in sheep [9]. Protein kinase A (PKA) and exchange protein directly activated by cAMP (Epac), a guanine nucleotide exchange factor, are two principal effectors of cAMP, are expressed in a wide range of tissues and control diverse biological functions. According to recent evidence, Epac and PKA might play independent, synergistic, or opposite roles in specific cellular functions [10]. The development of the specific Epac activator and cAMP analog 8-(4-chlorophenylthio)-2′-O-methyl-adenosine-3′,5′-cyclic mono-phosphate (8CPT) and the selective

Abbreviations: ALI, acute lung injury; ARDS, acute respiratory distress syndrome; LPS, lipopolysaccharide; HPMVEC, human pulmonary microvascular endothelial cells; PKA, protein kinase A; Epac, AMP-responsive guanine nucleotide exchange factor; 8CPT, 8-(4-chlorophenylthio)-2′-*O*-methyl-adenosine-3′,5′-cyclic mono-phosphate; 6Bnz, N6-benzoyl-adenosine-3′,5′-cyclic monophosphate; PGE2, prostaglandin E2; KC, keratinocyte-derived cytokine; TNF-α, tumor necrosis factor-α

* Corresponding author.
E-mail address: tanghuifang@zju.edu.cn (H. Tang).
[1] Co-first authors.

https://doi.org/10.1016/j.biopha.2017.11.110
Received 29 July 2017; Received in revised form 4 November 2017; Accepted 20 November 2017
0753-3322/ © 2017 Elsevier Masson SAS. All rights reserved.

PKA activator N6-benzoyl-adenosine-3′,5′-cyclic monophosphate (6Bnz) [14] enable the separate study of PKA- and Epac-mediated pathways. Therefore, in this study, we initially used *in vitro* models of LPS-induced lung injury to determine the effects of Epac and PKA and confirmed that an Epac activator plays a more important role in LPS-induced production of mediators of the early inflammatory response, such as TNF-α. We then used the Epac activator 8CPT by intratracheal instillation of LPS to induced lung injury in mice. The results suggested that 8CPT decreases the production of early-response cytokines, such as TNF-α, IL-1β, IL-6, and keratinocyte-derived cytokine (KC). Moreover, 8CPT improves lung injury and decreases microvascular leakage; the mechanism involves Rac1/2 but not the mitogen-activated protein kinase (MAPK) pathway. In summary, Epac plays an important role in modulating LPS-induced ALI. Epac activation reduces inflammation and microvascular permeability; therefore, a Epac activator represents a novel choice for the early therapy of ALI or ARDS.

2. Materials and methods

2.1. Information about drugs, reagents, cells and animals

LPS (*Escherichia coli* LPS O55:B5), the Epac activator (8-CPT-2 Me-cAMP [8-CPT]), the PKA activator (6-Bnz-cAMP [6BnZ]), and *o*-dianisidinedihydrochloride were purchased from Sigma-Aldrich (St. Louis, MO, U.S.A.). The Epac inhibitor ESI-09 was purchased from Selleck (Qingdao, Sandong, China), and the dexamethasone (Dex) injection was purchased from Zhejiang Xianju Pharmaceutical Co., Ltd. (Xianju, Zhejiang, China). TNF-α, IL-6, KC and IL-1β ELISA kits were purchased from R&D Systems (Minneapolis, MN, U.S.A.). The mouse albumin ELISA kit was purchased from Bethyl Laboratories (Montgomery, TX, U.S.A.). The mouse cAMP ELISA assay kit was purchased from R&D Systems. The Bio-Rad DC protein assay kit was purchased from Bio-Rad Laboratories (Hercules, CA, U.S.A.).

The mouse alveolar macrophage-derived cell line MH-S (CRL-2019) and the murine alveolar epithelial cell line MLE-12 (CRL-2110) were purchased from the American Type Culture Collection (Manassas, VA, U.S.A.). Human primary pulmonary microvascular endothelial cells (HPMVECs) and ECM cell culture medium were purchased from Sciencell (Walkersville, MD, U.S.A.). Eight-week-old male C57/B6 mice were obtained from the SLAC Laboratory Animal (Certificate No: SCXK2015-0016, Shanghai, China). The experimental protocols were approved by the Animal Care Committee of Zhejiang University in accordance with international guidelines.

2.2. Measurement of cytokine release from co-culture with alveolar macrophages and epithelial cells

MH-S cells were cultured in RPMI-1640 medium supplemented with 2 mM L-glutamine (Corning Life Sciences, Manassas, VA, USA), 10 mM HEPES, 100 U/ml penicillin, 100 U/ml streptomycin, and 10% (v/v) fetal bovine serum (Corning Life Sciences). MLE-12 cells were cultured in RPMI-1640 medium supplemented with 2 mM L-glutamine, 100 U/ml penicillin, 100 U/ml streptomycin, and 3% (v/v) fetal bovine serum). The cells were grown in a humidified incubator at 37 °C with 5% CO_2. MH-S cells were plated in 48-well plates (1×10^4 cells/well) overnight, pretreated with 10 μM 8CPT and 6BnZ for 5 min, and then stimulated with or without LPS (500 ng/ml). MLE-12 cells were added with a density of 1×10^4 cells per well. The supernatants were harvested 3, 12, 24 h after stimulation and stored at −80 °C. TNF-α levels were measured by using a Duoset ELISA kit (R&D Systems, Minneapolis, MN, U.S.A.).

To further investigate the effect of Epac, we treated MHS cell with Epac1 over-expressed plasmids (pCMV-Flag-RAPGEF3, Biogot Technology Co. Nanjing, China) or Epac1 siRNA (SANTA CRUZ, sc-41700). Before transfection, MHS cells were placed on 12-well plates and incubated until 70–80% confluent. Using jetPRIME transfection reagent (Polyplus-transfection, New York, USA), Epac1 expression plasmids (0.5 μg/ml, 1 μg/ml, 2 μg/ml) were transfected into MHS cell. After transfection 24 h, the cells were treated with 100 ng/ml LPS, control cell transfected with pCMV empty vector and treated with medium or LPS100 ng/ml. After 4 h, the supernatant were harvested for TNFα ELISA. To knockdown Epac1, by using INTERFER in transfection reagent (PolyPlus-transfection, New York, USA) 0.5 nM, 1 nM, 2 nM siRNA were transfected into MHS cell, after 36 h, the cells were treated with 100 ng/ml LPS, control cell treated with medium or LPS 100 ng/ml. After 4 h, the supernatant were harvested for TNFα ELISA.

2.3. Transendothelial permeability of HPMVECs

We used HPMVECs to further investigate the permeability of pulmonary endothelial cells and determined the FITC-Dextran content using previously described methods [15]. HPMVECs were cultured in ECM media (sciencell) supplemented with 5% FBS, maintained at 37 °C in a humidified atmosphere of 5% CO_2/95% air, and used at passages 6–7. HPMVECs were seeded on top of the transwell chamber (0.8-μm pore size, Costar, Cambridge, MA, U.S.A.) in 12-well plates and grown to confluence. The monolayer was serum-starved for 1 h and then incubated with fresh culture medium. 8-CPT or 6nBZ were added to the experimental medium at a final concentration of 100 μM in the presence or absence of 1 μg/ml LPS (0.5 ml in the upper chamber and 1.5 ml in the lower chamber), and the plate was incubated in a CO_2 incubator. After 24 h, the medium was replaced with 0.5 ml of HBSS containing FITC-Dextran (70 kD, final concentration: 1.0 mg/ml) into the upper chamber, and 1.5 ml of HBSS was added to the lower chamber. After incubation for 1 h, the transwell insert was removed, and 100 μl of medium from the lower chamber was collected. The fluorescent intensity was analyzed on a microplate fluorometer (Titertek Fluoroskan II, Lorton, VA, U.S.A.) at excitation and emission wavelengths of 485 and 530 nm, respectively.

2.4. LPS-induced ALI in mice

LPS-induced ALI was performed as previously described [3]. Briefly, before the experiment, the mice were fasted overnight. The animals were anesthetized with an intraperitoneal injection of 4% chloral hydrate at a dose of 280 mg/kg. A tracheostomy was performed, and 30 μl of saline containing LPS (2 ng/g) was slowly instilled intratracheally. Sham-treated animals received the same volume of saline alone. 8CPT (10 mg/kg, intravenous (iv) injection) and Dex (5 mg/kg) were injected intraperitoneally 5 min after LPS was administered. The animals were maintained at 37 °C until they recovered from the anesthesia. Six hours later, the mice were sacrificed, and samples were collected. After a 6-h exposure to LPS, the left lung of each mouse was lavaged with 0.5 ml of ice-cold, sterile PBS, and the amount of fluid recovered was routinely ≥90%. The bronchoalveolar lavage fluid (BALF) was used to determine the total leukocyte count and differential cell counts. Cell-free supernatant was used to measure the total protein and albumin levels using the above-mentioned kits.

2.5. Myeloperoxidase (MPO) activity

MPO activity was determined using previously described methods [16]. Enzymatic activity was determined spectrophotometrically by measuring the kinetics of absorbance at 450 nm over a 3-min period using a plate reader (Beckman Multimode Detector, DTX880, Brea, CA, U.S.A.). For detection, lung homogenates were centrifuged at 2000 × *g* and 4 °C for 10 min. The protein concentrations in homogenates were determined as described above.

2.6. Histological examination of the lung

The lower left lobe was fixed with 10% neutral formalin for 24 h to

Table 1
Primer sequence used for qPCR analysis.

Name	Sequence
mTNF-α-F	CATCTTCTCAAAATTCGAGTGACAA
mTNF-α-R	TGGGAGTAGACAAGGTACAACCC
mIL-1β-F	GCCCATCCTCTGTGACTCAT
mIL-1β-R	AGGCCACAGGTATTTTGTCG
mIL-6-F	TAGTCCTTCCTACCCCAATTTCC
mIL-6-R	TTGGTCCTTAGCCACTCCTTC
mKC-F	CATAGCCACACTCAAGAATGGT
mKC-R	TGAACCAAGGGAGCTTCAG
mβ-actin F	GAT TAC TGC TCT GGC TCC TAG C
mβ-actin R	GAC TCA TCG TAC TCC TGC TTG C

characterize the histological alterations. Paraffin sections (4 μm) were prepared, and hematoxylin and eosin staining was performed to evaluate lung edema and inflammatory cell infiltration. The degree of lung injury was evaluated based on the scoring system described in an Official American Thoracic Society Workshop report [17]. The evaluation was performed by a pathologist who was blinded to the experimental groups using an Olympus CX31 microscope.

2.7. Real-time quantitative PCR (qPCR) analysis

Total RNA from lung tissues was isolated using RNAiso^{TM} Plus (TaKaRa, Japan), and first-strand cDNAs were synthesized using Moloney murine leukemia virus (M-MLV) reverse transcriptase (TaKaRa, Japan). The mRNA levels were measured by qPCR using a LightCycler 480 SYBR Green I Master Mix (Roche, Switzerland) with a LightCycler 480 machine. Glyceraldehyde 3-phosphate dehydrogenase (GAPDH) and β-actin were used as housekeeping genes. The sequences of the primers used for qPCR analyses are shown in Table 1. The qPCR program consisted of an initial step at 95 °C for 10 min followed by 45 cycles of 95 °C for 10 s, 60°C for 20 s, and 72 °C for 30 s. The specificity of the amplified products was verified using dissociation curves. Quantification of the relative levels of the target genes in different tissues was performed by calculating the threshold cycle (Ct) value using the $2^{-\triangle\triangle T}$ method.

2.8. Western blot analysis

Proteins in lung extracts were prepared in radioimmunoprecipitation assay (RIPA) buffer (1% Triton X-100, 1% deoxycholate, and 0.1% SDS, Boster, China) containing 1× PhosSTOP (Roche, Switzerland), a 1% protease inhibitor cocktail (Roche, Switzerland), and 2% PMSF (Sigma, USA). Samples containing 50 μg of proteins were electrophoresed on a 10% gradient SDS-PAGE gel and transferred to nitrocellulose (NC) membranes (Schleicher & Schuell) using a Mini-PROTEAN II system (Bio-Rad Laboratories, Hercules, CA, U.S.A.). The membranes were incubated with TBS containing 5% nonfat milk or bovine serum albumin (BSA) for 1 h at room temperature to block nonspecific binding sites. The membranes were incubated with the following antibodies overnight at 4 °C: mouse anti-Epac1 (Cell Signaling Technology, #4155, 1:1000), rabbit anti-PKAγ (Abcam, ab 108385, 1:500), rabbit anti-PKAα + β (Abcam, ab 71764, 1:500), rabbit anti-phosphorylated PKAα + β (Abcam, ab 59218, 1:500), and mouse anti-β-actin (Santa Cruz Biotechnology, sc-47778, 1:4000). The membranes were then incubated with the secondary antibody at a dilution of 1:3000 (IRDye 800CW goat anti-rabbit IgG; IRDye 680CW goat anti-mouse, LI-COR) for 1 h at room temperature and imaged with the LI-COR Odyssey infrared imaging system. The bands were quantified using Quantity One software (Bio-Rad).

2.9. Analysis of MAPK phosphorylation

For the semi-quantitative measurement of extracellular signal-regulated kinase (ERK) 1/2 (pT202/Y204), p38 MAPK (pT180/Y182) and c-Jun N-terminal kinase (JNK) 1/2/3 (pT183/Y185) concentrations in protein extracts, we purchased PhosphoTracer assay kits (ab 119674, Abcam) to detect the endogenous levels of ERK 1/2 (GenBank Accessions NP 002737.2 [ERK1] and NP 620407 [ERK2]), JNK 1/2/3 (GenBank Accessions NP_620637 [JNK1], NP_620707 [JNK2] and NP_620446 [JNK3]), and p38 MAPK (GenBank Accession NP_001306) in lung lysates. These assays detect the level of each MAPK protein when phosphorylated at the conserved activation site of each respective protein. For the PhosphoTracer assays, both assay reagents were simultaneously added to the PhosphoTracer assay microplate. After a short incubation period, any unbound assay reagents and analysts were washed away, and immune complexes containing both antibodies were detected. The fluorescence signal was measured with a PhosphoTracer-compatible filter set.

2.10. Pull-down assay for Rac1, Rac2, Cdc42 and RhoA activities

Rac1, Rac2, Cdc42 and RhoA activation assays were performed using Rac1, Rac2, Cdc42 and RhoA activation assay kits (R&D Systems), respectively. Briefly, after 50 mg (wet weight) of lung tissues were minced and sonicated in 1× lysis buffer, the sample was centrifuged at 150,000*g* for 15 min. The supernatant was harvested for the Rac1, Rac2, Cdc42 or RhoA activation assays, according to the manufacturer's standard protocol. Active forms (GTP-bound forms) of Rac1, Rac2, Cdc42 or Rho were detected by Western blotting, and a semi-quantitative analysis was performed using ImageJ software (NIH, http://rsb.info.nih.gov/ij/download.html). β-Actin was used as an internal control for the total Rac1, Rac2, Cdc42 and Rho levels.

2.11. Statistical analysis

The results are reported as the means ± standard errors of the means (SEM). One-way ANOVA was used to compare the means of specific groups, and $p < 0.05$ was considered to indicate significance. All analyses were performed using GraphPrism5 software.

3. Results

3.1. Epac activation reduced the release of pro-inflammatory cytokines

Epac and PKA are cAMP effectors, but researchers have not determined which protein plays the more important role in LPS-induced inflammation. 8CPT is the Epac activator, ESI-09 is a novel Epac-specific antagonist, H89 is the PKA inhibitor, and 6-Bnz is the PKA-selective agonist. In the current study, we first investigated the effect of Epac/PKA activators and inhibitors on LPS-induced inflammation in macrophages and epithelial cells. We used the LPS-stimulated MH-S macrophage cell line and MLE-12 epithelial cell line, to determine the amount of TNF-α released from MH-S cells and co-cultures with MLE-12 cells. TNF-α is the most important inflammatory cytokine produced by macrophages. TNF-α secretion was only significantly reduced by 8CPT, whereas the PKA activator 6nBz did not have a significant effect on LPS-induced TNF-α secretion at all time points compared with control MH-S cells (Fig. 1A). Moreover, TNF-α was produced at similar levels in LPS-stimulated MH-S and co-cultures with MLE-12 cells, a significant decrease was only observed with the 8CPT treatment after 12 h (Fig. 1A). Based on these data, 8CPT inhibits the release of this cytokine from lung macrophages and epithelial cells. Thus, Epac, but not PKA, regulates the production of pro-inflammatory cytokines in LPS-induced ALI.

To support the importance of Epac-regulated inflammation signaling,we further transiently depleted Epac with siRNA or over-expressed Epac1 in MHS cell (Fig. 1B), then found that Epac-siRNA push a little

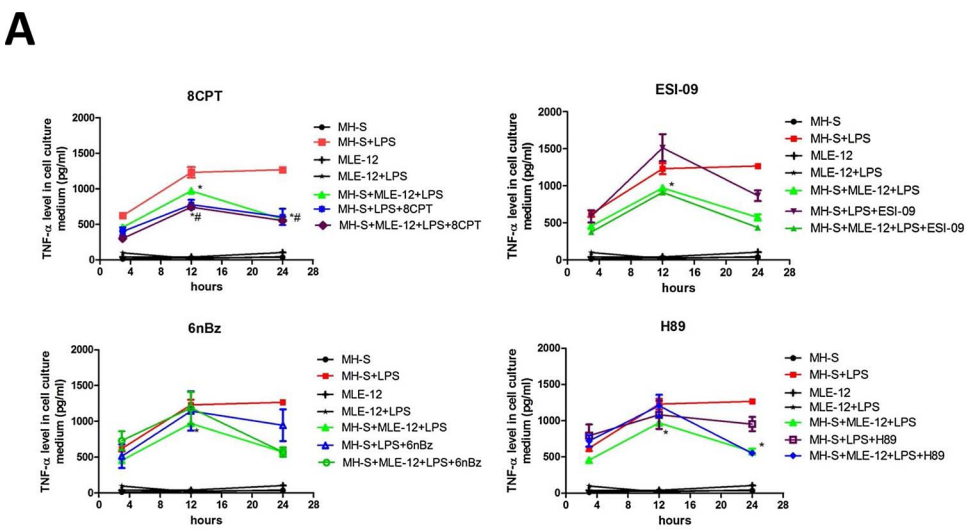

Fig. 1. 8CPT reduced cytokine/chemokine secretion in culture supernatants. MH-S or MLE-12 cells were stimulated with 500 ng/ml LPS, and ESI-09, 8CPT, H-89, and 6nBZ were added immediately after LPS administration. The supernatant was harvested at 3, 12, or 24 h after LPS administration. (A) Effects of ESI-09, 8CPT, H-89, and 6nBZ (10 μM) on TNF-α release from LPS-stimulated MH-S cells, MLE-12 cells or co-cultures. The results are presented as the means ± SEM (n = 6). $*p < 0.05$ $**p < 0.01$, $***p < 0.001$ compared with LPS alone. (B) Effects of Epac1 expressed plasmids (0.5 μg/ml, 1 μg/ml, 2 μg/ml) and Epac siRNA (0.5 nM, 1 nM, 2 nM) on TNF-α release from LPS-stimulated MH-S cells. The results are presented as the means ± SEM (n = 6). $*p < 0.05$ $**p < 0.01$, $***p < 0.001$ compared with LPS alone.

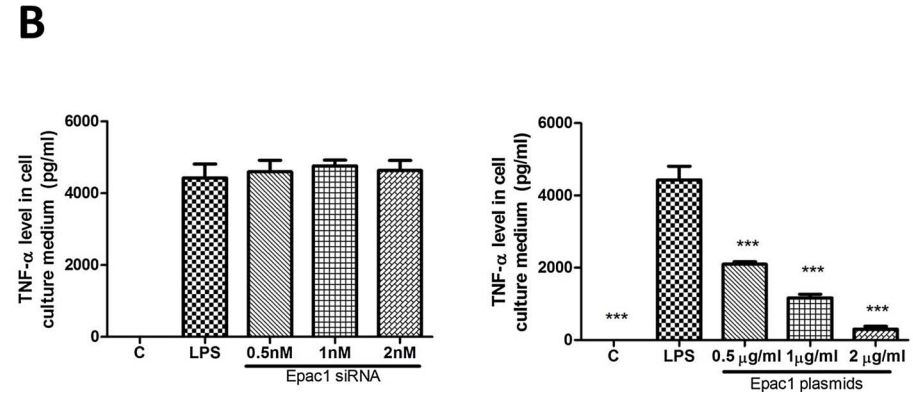

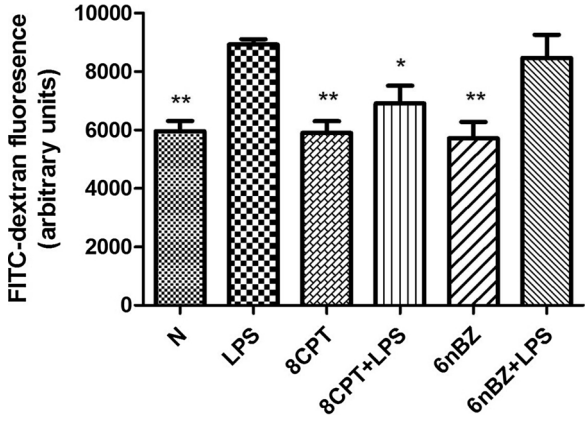

Fig. 2. LPS-induced HPMEC barrier dysfunction was assessed by measuring FITC-dextran leakage. HPMECs were stimulated with 1 μg/ml LPS, and the Epac or PKA activator (10 μM) was added immediately after LPS administration. Twenty-four hours later, the medium in the lower chamber was harvested after the addition of HBSS containing FITC-dextran. The results are presented as the means ± SEM (n = 5). $*p < 0.05$, $**p < 0.01$, $***p < 0.001$.

higher degree of inflammation induced by LPS, while Epac plasmids significant suppress the inflammation induced by LPS. Thus, our data strongly supported that Epac regulates the production of pro-inflammatory cytokines in LPS-induced ALI.

3.2. Epac activation reduced LPS-induced vascular permeability in the lung

We determined the FITC-Dextran content in the lower chamber after LPS exposure to further investigate the effects of Epac and PKA activation on the permeability of pulmonary endothelial cells. LPS induced a more than 1.7-fold increase in FITC-Dextran exudation. The Epac activator 8CPT decreased the FITC-Dextran exudation by 57% (Fig. 2). However, no significant difference was observed in the 6nBZ group. Thus, LPS-induced endothelial permeability is mediated by Epac and not PKA.

3.3. The Epac activator suppressed LPS-induced murine lung inflammation

Based on the results described above, we speculated that the Epac activator might be a novel therapy for ALI. Therefore, we further evaluated the effect of the Epac activator 8CPT on an animal model of LPS-induced lung injury. Six hours after the instillation of LPS, we collected the BALF and lung tissues. Lung histology revealed a dramatic increase in neutrophil infiltration in the lungs after LPS instillation (Fig. 3A & B). In mice treated with the Epac activator 8CPT, the characteristic changes were markedly suppressed, and neutrophil accumulation in the lungs was substantially decreased. Dex-treated mice exhibited a similar decrease. The total number of leukocytes in the BALF was counted to further examine neutrophil migration. The total number was increased by ~6.9-fold in mice with LPS-induced injury compared with control mice ($p < 0.001$). Furthermore, compared with mice with LPS-induced injury alone, the total number of leukocytes in 8CPT-

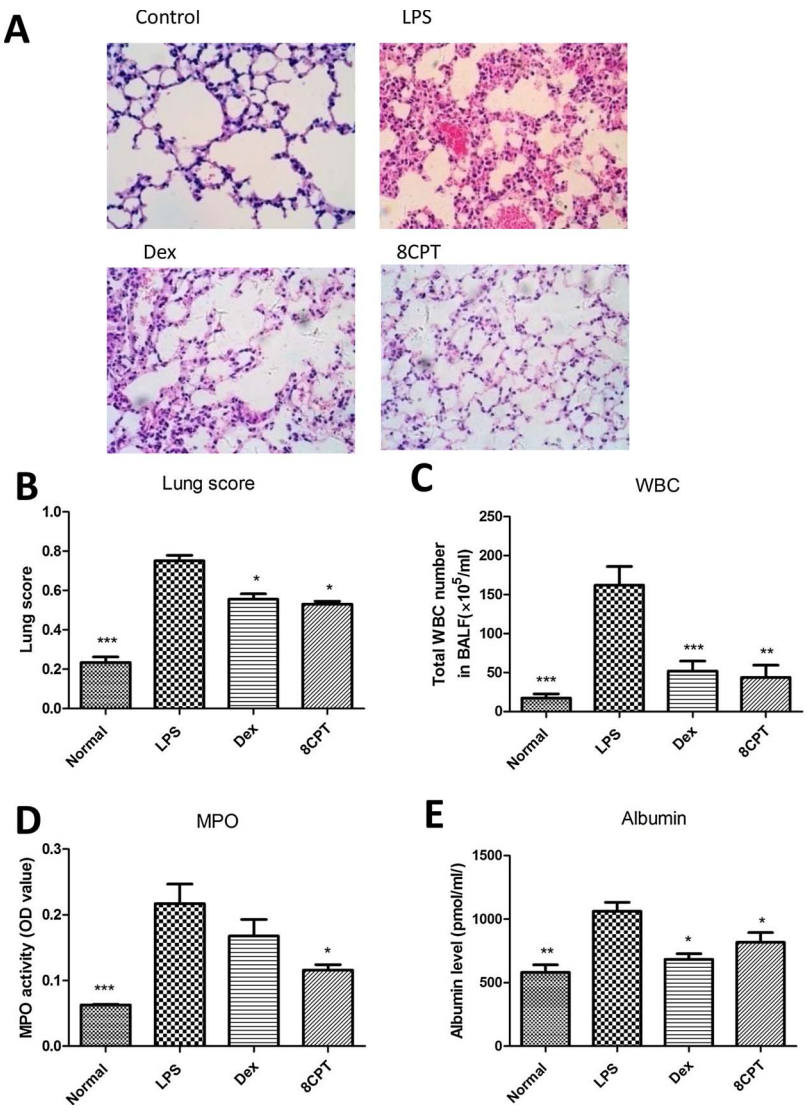

Fig. 3. 8CPT mitigated lung inflammation and neutrophil infiltration in mice after LPS-induced lung injury. Whole lungs and BALF were harvested 6 h after treatment with 2 mg/kg LPS. (A) Representative images of hematoxylin and eosin (H&E)-stained paraffin-embedded lung sections harvested from control, LPS-, 8CPT-, and Dex-treated mice. Original magnification, ×400. (B) Lung injury scores. (C) Total number of leukocytes in the BALF. (D) MPO activity in lung homogenates. (E) Albumin leakage in the BALF. The results are presented as the means ± SEM (n = 10). $^{*}p < 0.05$, $^{**}p < 0.01$, $^{***}p < 0.001$ compared with LPS alone.

treated LPS-injured mice was decreased by 64% ($p < 0.001$), and Dex decreased the count by 62% (Fig. 3C). MPO activity indicates the lung neutrophil burden and exhibited a significant reduction after treatment with 8CPT and Dex (Fig. 3D). Based on our data, Epac activation markedly attenuated LPS-induced pulmonary inflammation and decreased neutrophil migration. These findings were consistent with the *in vitro* results and confirmed that the Epac activator ameliorated LPS-induced inflammation. Thus, this compound might represent an effective therapy for ALI.

3.4. The Epac activator reduced LPS-induced vascular permeability in the lung

We detected the albumin levels in the BALF, which could indicate a compromised endothelial/epithelial alveolar cell barrier, to further confirm the effect of 8CPT on pulmonary vascular permeability. LPS exposure induced an evident increase in vascular permeability. Notably, the albumin permeability index was significantly decreased in 8CPT-treated mice compared with mice treated with LPS mice and Dex-treated mice (Fig. 3E). These findings were also consistent with the *in vitro* results and confirmed that the Epac activator affected vascular permeability.

3.5. The Epac activator inhibited cytokine/chemokine expression in the lung

We harvested the lungs 6 h after the intratracheal administration of LPS to further confirm the effects of 8CPT on pro-inflammatory cytokine/chemokine production. Only very low levels of inflammatory cytokine/chemokine mRNAs were detected in the lungs of control mice. Notably, in LPS-injured mice, 8CPT and Dex significantly decreased the levels of TNF-α, IL-6, KC, and IL-1β mRNAs (Fig. 4). These findings were also consistent with the *in vitro* results and confirmed that Epac plays a special role in the generation of cytokines/chemokines in the lung during LPS-induced ALI through a mechanism similar to that of glucocorticoids.

3.6. Epac inhibition was involved in LPS-induced murine lung inflammation

We investigated known downstream substrates of cAMP, PKA and Epac, to further investigate the downstream cAMP signaling pathway responsible for the effects of LPS. LPS significantly decreased Epac expression ($p < 0.05$), but the levels of total and phosphorylated PKA were not significantly changed. 8CPT exhibited detectable inhibitory effects and increased Epac expression but did not change PKA expression or phosphorylation (Fig. 5). Thus, the major effector of LPS-induced lung injury was Epac ($p < 0.001$ compared with LPS). Interestingly, Dex significantly increased the expression of Epac1 protein, suggesting a new anti-inflammatory mechanism of glucocorticoids.

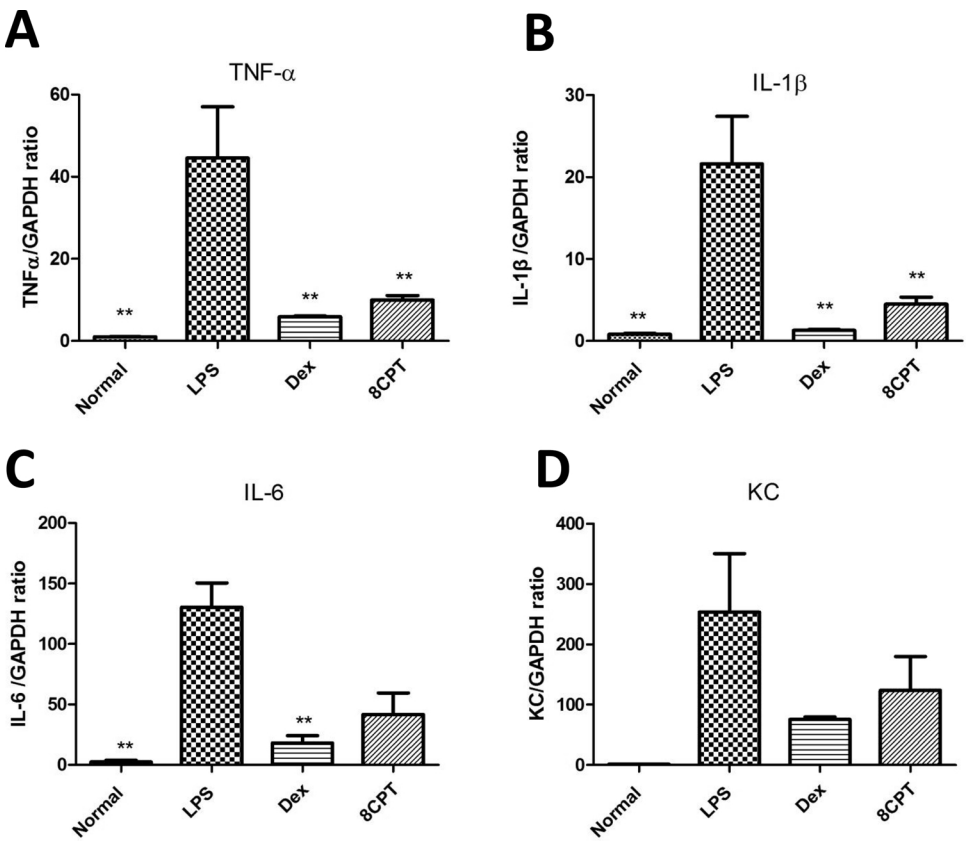

Fig. 4. 8CPT reduced the expression of inflammatory cytokine mRNA in the lung. Lungs were harvested 6 h after treatment with 2 mg/kg LPS. (A) TNF-α, (B) IL-1β, (C) IL-6, and (D) KC. The results are presented as the means ± SEM (n = 5). $^{*}p < 0.05$, $^{**}p < 0.01$, $^{***}p < 0.001$ compared with LPS alone.

3.7. The Epac activator did not affect the LPS-induced inflammatory response via the MAPK pathway

We determined the phosphorylation status of members of the MAPK pathway to further investigate the signaling pathway downstream of Epac (Fig. 6). Based on our results, the p38 MAPK pathway was unchanged after LPS exposure, whereas the ERK and JNK MAPK pathways were significantly activated. Dex and 8CPT did not affect the JNK MAPK pathway, but Dex and not 8CPT significantly decreased the phosphorylation of the ERK pathway ($p < 0.05$). Thus, the Epac activator does not use the MAPK pathway to suppress inflammation.

3.8. The Epac activator inhibited the LPS-induced inflammatory response via small GTPases

We further examined the guanine nucleotide exchange factor (Epac or cAMP-GEF)-activated small GTPases Rac1/2, RhoA and Cdc42 as a continuation of our search for the downstream molecular pathway. Rac1/2 and Cdc42 activities were increased in whole-lung extracts after LPS exposure; 8CPT decreased Rac1 and Cdc42 activities to the baseline levels (Fig. 7A). RhoA was unchanged after LPS exposure, and 8CPT had no effect on RhoA activity. Rac1 activation regulates the endothelial barrier. Therefore, based on these results, the Epac activator might change the endothelial barrier by inhibiting Rac1/2 activation. Further studies are needed to confirm this relationship and determine the complex post-transcriptional regulatory mechanism (Fig. 8).

4. Discussion

Based on our data, (1) the Epac activator 8CPT reduces the early phase of LPS-induced inflammation in macrophages and epithelial cells. (2) The Epac activator 8CPT reduces the LPS-enhanced microvascular permeability. (3) Epac expression is down-regulated in LPS-induced lung injury. (4) The Epac activator 8CPT exerts a protective effect on LPS-induced ALI. (5) The mechanism through which the Epac activator ameliorates LPS-induced lung injury involves Rac1/2. Therefore, 8CPT exerts an anti-inflammatory effect on the early phase of LPS-induced lung injury.

PKA and Epac are two principal effector proteins involved in cAMP signaling; they are expressed in a wide range of tissues and control diverse biological functions [10]. The existence of two cAMP effectors provides more precise regulation of cAMP signaling pathways in different spatiotemporal manners. Recently, Epac and PKA were suggested to play independent, synergistic or opposite roles in a specific cellular function. For example, hyperoxia-induced BDNF (brain-derived neurotrophic factor) secretion in developing airway smooth muscle was found to be Epac2-dependent, whereas PKA inhibition does not influence this process [18]. PKA exclusively mediates the inhibitory effects of prostaglandin E2 (PGE2) on collagen I expression; however, Epac1 exclusively inhibits fibroblast proliferation [19]. Moreover, endothelial nitric oxide (NO) release mediates vascular relaxation through the synergistic activation of PKA and Epac [20]. As shown in our study, LPS induces lower Epac1 and Epac2 expression but has no impact on PKA. Cigarette smoke extract (CSE) decreases Epac1 expression but does not affect Epac2 and PKA expression [21,22]. Findings from these previous studies were consistent with the results from our study and suggest that reduced Epac1 expression might be the common phenomenon in inflammation.

Epac and PKA also exert different effects on LPS-induced inflammation. LPS-stimulated NO production in murine BV2 microglial cells has been shown to primarily depend on PKA because Epac1-mediated Rap1 activation is not required for the induction of NO production [23]. Although 8CPT increases NF-κB activity in LPS-treated RAW 264.7 murine macrophages, NF-κB is also activated by cAMP production through Epac1-mediated Rap1 activation [24]. Activation of Epac with 8CPT didn't inhibit LPS-induced increases in TNF-α mRNA levels in J774 and RAW 264.7 macrophages, whereas the activation of PKAI with 6BnZ inhibited by 50% [25]. However, conflicting evidence

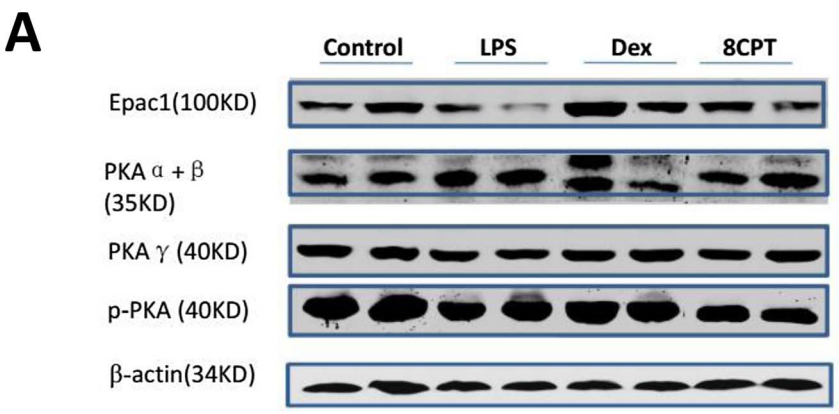

Fig. 5. Changes in Epac and PKA signaling pathways in LPS-induced lung injury. (A) Western blots of Epac, PKA, and phosphorylated PKA protein levels in LPS-injured lungs. As described above, lung tissues were homogenized in lysis buffer, and the samples were then subjected to Western blot analysis. The levels of Epac, PKAα/β, PKAγ, and phosphorylated PKA proteins were detected using subtype-specific polyclonal antibodies. β-actin served as a loading control. (B) Densitometric quantification of the levels of Epac, PKAα/β, PKAγ, and phosphorylated PKA proteins from the Western blots. The values are presented as the means ± SEM (n = 2). $*p < 0.05$, $**p < 0.01$, $***p < 0.001$.

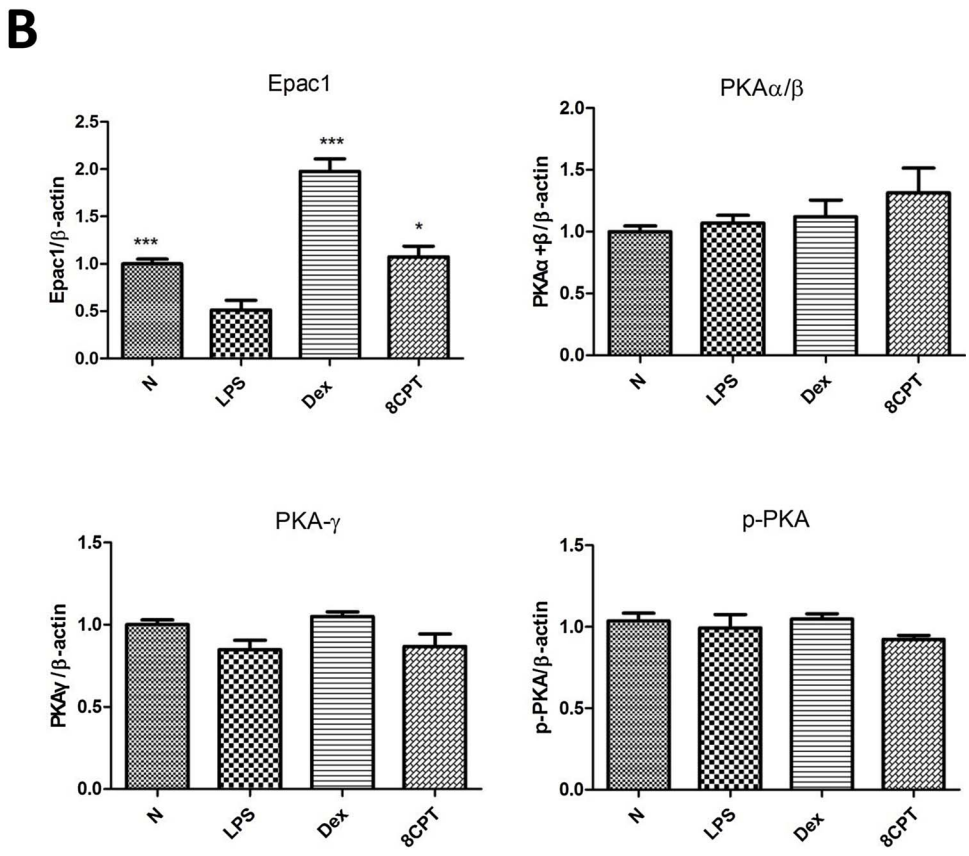

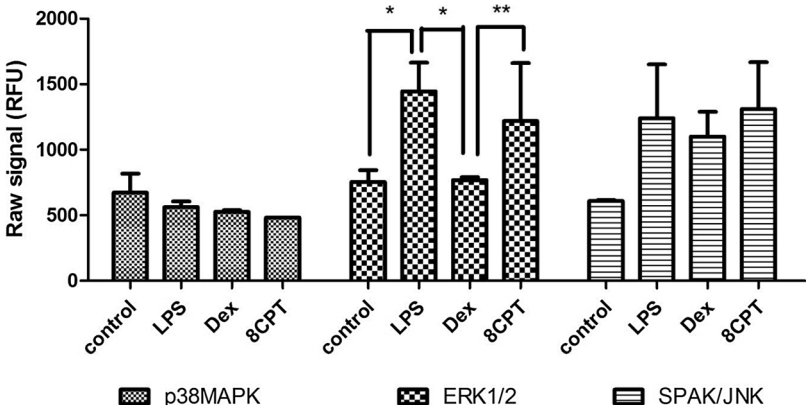

Fig. 6. Changes in the MAPK signaling pathway in LPS-induced lung injury. The p38 MAPK pathway was not changed after LPS exposure, whereas the ERK and JNK MAPK pathways were significantly activated. Dex and 8CPT did not affect the JNK MAPK pathway, but Dex and not 8CPT significantly decreased ERK phosphorylation ($p < 0.05$). The values are presented as the means ± SEM (n = 6). $*p < 0.05$, $**p < 0.01$,$***p < 0.001$.

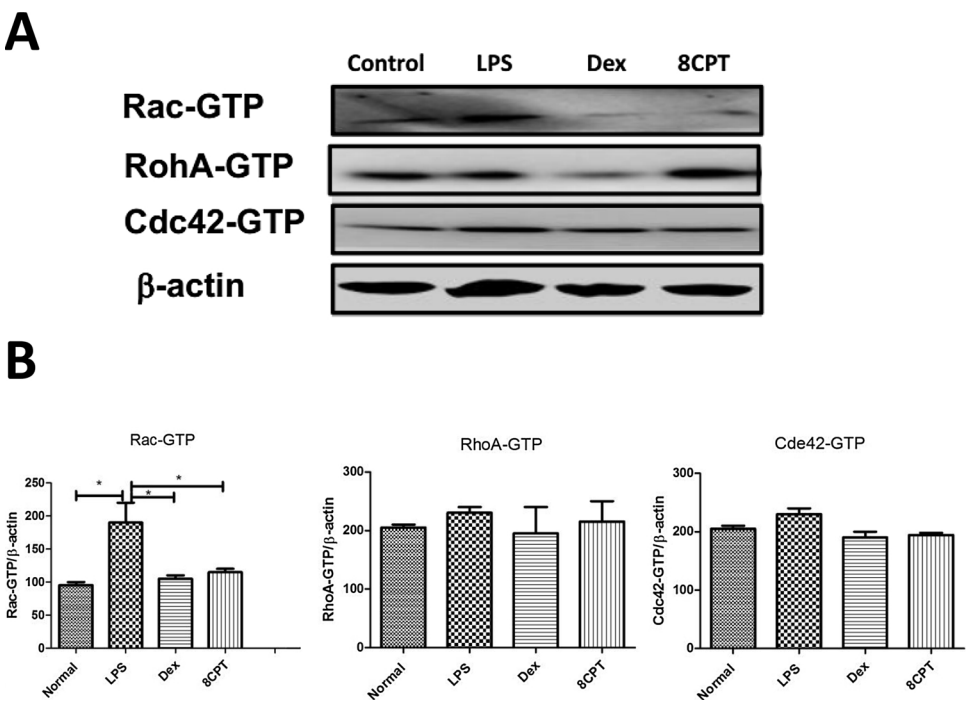

Fig. 7. 8CPT reduced Rac and Cdc42 activation in the lungs of mice with LPS-induced ALI. (A) Results of the activated Rac, RhoA and Cdc42 pull-down assays. β-Actin was used as an internal control. Lungs were harvested from control, LPS-, Dex- and 8CPT-treated LPS-injured mice 6 h after LPS instillation. (B) Densitometric quantification of Rac1, Rho, and Cdc42 levels in the lung was performed as described above. The values are presented as the means ± SEM (n = 2). $^{*}p < 0.05$, $^{**}p < 0.01$, $^{***}p < 0.001$.

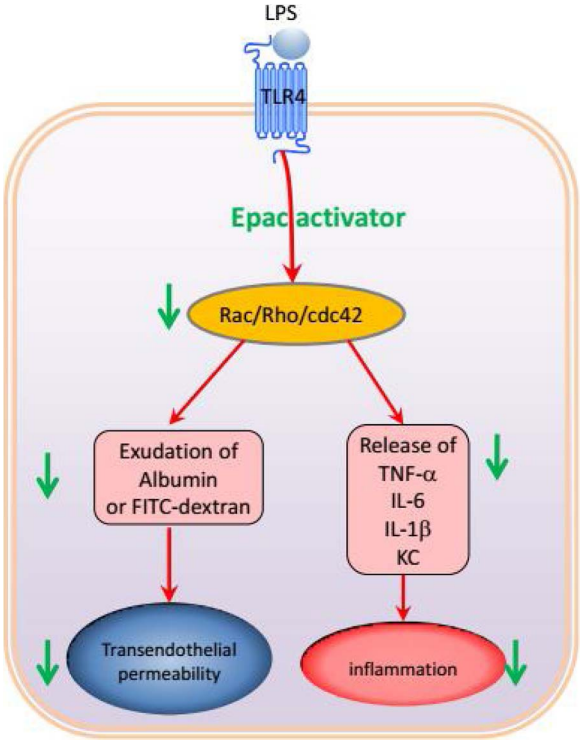

Fig. 8. Rac/Rho/Cdc42 pathways are activated in response to LPS stimulation and contribute to the production of pro-inflammatory mediators and transendothelial permeability. 8CPT, a novel cAMP analogue, inhibits LPS-induced activation of Rac/Rho/Cdc42 signaling pathways, attenuating inflammatory responses.

has also been reported. In CSE-induced inflammation in human airway smooth muscle (ASM) cells, 8CPT prevents CSE-induced p65 nuclear translocation and subsequently decreases CSE-induced IL-8 release [21].

Our study provides the first indication that 8CPT inhibits TNF-α release from MH-S cell (Fig. 1A) and the expression of cytokine mRNAs in LPS-induced lungs (Fig. 3). The results obtained with the co-culture system further confirm the effects of 8CPT on epithelial cells and macrophages. Based on the animal experiments, 8CPT exerts an anti-inflammatory effect on LPS-induced lung injury, significantly decreases the number of white blood cells (WBC) in the BALF (Fig. 2C), decreases MPO activity (Fig. 2D), up-regulates the LPS-induced down-regulation of Epac1 expression in whole lung (Fig. 5), and inhibits activation of small GTPases, such as Rac (Fig. 6), but does not affect the MAPK pathway (Fig. 5). Although we did not determine the precise mechanism governing the effects of 8CPT on LPS-induced ALI, our data indicate that PKA activation does not decrease the levels of pro-inflammatory mediators after 6 h of LPS stimulation (Fig. 1A) but did have an effect on endothelial permeability (Fig. 1B). Moreover, in the present study, we did not assess the *in vivo* effect of the Epac inhibitor ESI-09. However, according to a recent report, ESI-09 inhibits complete Freund's adjuvant-induced mechanical hyperalgesia [26], further suggesting that an Epac inhibitor might be a potential therapeutic target for other diseases.

All these conclusions depend on pharmacological activators and inhibitors of Epac and PKA. Nonetheless, the drugs used in this study are not perfect. Some questions have been raised regarding these activators/inhibitors. 8CPT is a strong Epac activator and is even stronger than cAMP, but it exhibits weak activation and lower affinity for PKA. Simultaneously, 8CPT is also a good substrate for both PDE5 and PDE10 and can act as an inhibitor of PDE1, 2 and 6 [27,28]. The inhibitor of Epac ESI-09 has been shown to act as a chemical with general protein-denaturing properties and does not selectively inhibit Epac [29]. H-89 might inhibit other kinases in addition to PKA [10]; 6BnZ is a preferential PKA activator and is the most PKA-selective and PDE-resistant cAMP analogue [28]. We have shown a lack of an anti-inflammatory effect on the PKA-dependent pathway, but this compound is likely to have effects on other pathway.

EC barrier dysfunction triggered by inflammatory mediators involves more than one mechanism, explaining the partial attenuation of EC barrier compromise obtained with PKA and Epac activators. PKA-dependent phosphorylation of vasodilator-stimulated phosphoprotein (VASP) has been shown to make a positive contribution to the cAMP-mediated protection from LPS-induced barrier compromise [30]. PKA-independent mechanisms of EC barrier enhancement mediated by the activation of Epac/Rap1/T cell lymphoma invasion and metastasis 1 (Tiam1)/Vav2/Rac cascades protect against thrombin-induced EC

hyperpermeability [31–33]. Furthermore, the Epac/Rap1 pathway has been shown to attenuate the platelet-activating factor (PAF)-induced acute increase in vascular permeability [34]. As shown in several previous studies, LPS-induced endothelial barrier dysfunction might be mediated by several pathways, one of which involves the activation of MAP kinases, but controversy regarding whether ERK1/2 or p38 is more important still exists [35]. Another critical mechanism is involved in the activation of Rho pathways, such as Rac/Cdc42 [36] and Rap1 [32]. Rac1 mediates peripheral cytoskeleton enhancement and the enlargement of adherens junction complexes in pulmonary endothelial monolayers [37–39]. Rac1 activation mediates endothelial barrier recovery after thrombin or LPS challenge [40,41]. However, a Rac1 inhibitor also exerts a protective effect on LPS-induced lung injury, and inhibit the inflammation and microvascular permeability [38]. So, Rac1 maybe have different character in different situation. In our study, Rac1 activation was increased throughout the LPS induced lung (Fig. 7). We have not identified the exact mechanism through which Epac activation regulates LPS-induced acute lung vascular barrier dysfunction, but we speculate that the possible target of Epac activators might be the direct stimulation of Rac1/2.

In summary as Fig. 8 the major finding of the current study is that activation of Epac by 8CPT effectively reduces LPS-induced inflammation and pulmonary vascular permeability, which suggests that Epac might play important physiological roles as signals for pulmonary inflammation and vascular permeability. Regarding defective drugs, further studies that directly target Epac1/2 or PKA in LPS-induced ALI are needed. Based on our limited experimental data, we believe that more detailed work using Epac1- and Epac2-knockout mice might reveal the precise roles of Epac.

5. Conflict of interest

We declare that no financial and personal relationships with other people or organizations that inappropriately influenced our work exist. None of the authors have conflicts of interest regarding our work to report.

Acknowledgement

This research was supported by grants from the National Natural Science Foundation of China (Grant Nos: 81202980, 30800497, 81170536, 31400751 and 81570056).

References

[1] Y. Butt, A. Kurdowska, T.C. Allen, Acute lung injury: a clinical and molecular review, Arch. Pathol. Lab. Med. 140 (2016) 345–350.
[2] T.J. Standiford, P.A. Ward, Therapeutic targeting of acute lung injury and acute respiratory distress syndrome, Transl. Res. J. Lab. Clin. Med. 167 (2016) 183–191.
[3] H. Chen, C. Bai, X. Wang, The value of the lipopolysaccharide-induced acute lung injury model in respiratory medicine, Expert Rev. Respir. Med. 4 (2010) 773–783.
[4] H.F. Tang, J.J. Lu, J.F. Tang, X. Zheng, Y.Q. Liang, X.F. Wang, Y.J. Wang, L.G. Mao, J.Q. Chen, Action of a novel PDE4 inhibitor ZL-n-91 on lipopolysaccharide-induced acute lung injury, Int. Immunopharmacol. 10 (2010) 406–411.
[5] A.E. Taylor, Pulmonary edema: ischemia reperfusion endothelial injury and its reversal by c-AMP, Proc. Natl. Sci. Counc. Repub. China B 15 (1991) 191–195.
[6] K. Hsu, D. Wang, M.L. Chang, C.P. Wu, H.I. Chen, Pulmonary edema induced by phorbol myristate acetate is attenuated by compounds that increase intracellular cAMP, Res. Exp. Med. 196 (1996) 17–28.
[7] W.K. Adkins, J.W. Barnard, S. May, A.F. Seibert, J. Haynes, A.E. Taylor, Compounds that increase cAMP prevent ischemia-reperfusion pulmonary capillary injury, J. Appl. Physiol. 72 (1992) 492–497.
[8] A.F. Seibert, W.J. Thompson, A. Taylor, W.H. Wilborn, J. Barnard, J. Haynes, Reversal of increased microvascular permeability associated with ischemia-reperfusion: role of cAMP, J. Appl. Physiol. 72 (1992) 389–395.
[9] H. Hoffmann, J.R. Hatherill, J. Crowley, H. Harada, M. Yonemaru, H. Zheng, A. Ishizaka, T.A. Raffin, Early post-treatment with pentoxifylline or dibutyryl cAMP attenuates Escherichia coli-induced acute lung injury in guinea pigs, Am. Rev. Respir. Dis. 143 (1991) 289–293.
[10] K. Hsu, D. Wang, C.Y. Shen, C.H. Chiang, Protamine-induced acute lung injury and the protective effect of agents that increase cAMP, Proc. Natl. Sci. Counc. Repub. China B 17 (1993) 57–61.
[14] A.E. Christensen, F. Selheim, J. de Rooij, S. Dremier, F. Schwede, K.K. Dao, A. Martinez, C. Maenhaut, J.L. Bos, H.G. Genieser, S.O. Døskeland, cAMP analog mapping of Epac1 and cAMP kinase. Discriminating analogs demonstrate that Epac and cAMP kinase act synergistically to promote PC-12 cell neurite extension, J. Biol. Chem. 278 (2003) 35394–35402.
[15] N. Thorball, FITC-dextran tracers in microcirculatory and permeability studies using combined fluorescence stereo microscopy, fluorescence light microscopy and electron microscopy, Histochemistry 71 (1981) 209–233.
[16] P.P. Bradley, D.A. Priebat, R.D. Christensen, G. Rothstein, Measurement of cutaneous inflammation: estimation of neutrophil content with an enzyme marker, J. Invest. Dermatol. 78 (1982) 206–209.
[17] G. Matute-Bello, G. Downey, B.B. Moore, S.D. Groshong, M.A. Matthay, A.S. Slutsky, W.M. Kuebler, Acute Lung Injury in Animals Study Group, An official American Thoracic Society workshop report: features and measurements of experimental acute lung injury in animals, Am. J. Respir. Cell Mol. Biol. 44 (2011) 725–738.
[18] M.A. Thompson, R.D. Britt Jr., I. Kuipers, A. Stewart, J. Thu, H.C. Pandya, P. MacFarlane, C.M. Pabelick, R.J. Martin, Y.S. Prakash, cAMP-mediated secretion of brain-derived neurotrophic factor in developing airway smooth muscle, Biochim. Biophys. Acta 1853 (2015) 2506–2514.
[19] S.K. Huang, S.H. Wettlaufer, J. Chung, M. Peters-Golden, Prostaglandin E2 inhibits specific lung fibroblast functions via selective actions of PKA and Epac-1, Am. J. Respir. Cell Mol. Biol. 39 (2008) 482–489.
[20] V. García-Morales, A. Cuíñas, J. Elíes, M. Campos-Toimil, PKA and Epac activation mediates cAMP-induced vasorelaxation by increasing endothelial NO production, Vasc. Pharmacol. 60 (2014) 95–101.
[21] A. Oldenburger, S.S. Roscioni, E. Jansen, M.H. Menzen, A.J. Halayko, W. Timens, H. Meurs, H. Maarsingh, M. Schmidt, Anti-inflammatory role of the cAMP effectors Epac and PKA: implications in chronic obstructive pulmonary disease, PLoS One 7 (2012) e31574.
[22] A. Oldenburger, W. Timens, S. Bos, M. Smit, A.V. Smrcka, A.C. Laurent, J. Cao, M. Hylkema, H. Meurs, H. Maarsingh, F. Lezoualc'h, M. Schmidt, Epac1 and Epac2 are differentially involved in inflammatory and remodeling processes induced by cigarette smoke, FASEB J. 28 (2014) 4617–4628.
[23] E.Y. Moon, S.Y. Oh, G.H. Han, C.S. Lee, S.K. Park, Epac1-mediated Rap1 activation is not required for the production of nitric oxide in BV2, murine microglial cells, J. Neurosci. Res. 81 (2005) 38–44.
[24] E.Y. Moon, S. Pyo, Lipopolysaccharide stimulates Epac1-mediated Rap1/NF-kappaB pathway in Raw 264.7 murine macrophages, Immunol. Lett. 110 (2007) 121–125.
[25] J.B. Stafford, L.J. Marnett, Prostaglandin E2 inhibits tumor necrosis factor-alpha RNA through PKA type I, Biochem. Biophys. Res. Commun. 366 (2008) 104–109.
[26] P. Singhmar, X. Huo, N. Eijkelkamp, S.R. Berciano, F. Baameur, F.C. Mei, Y. Zhu, X. Cheng, D. Hawke, F. Mayor Jr., C. Murga, C.J. Heijnen, A. Kavelaars, Critical role for Epac1 in inflammatory pain controlled by GRK2-mediated phosphorylation of Epac1, Proc. Natl. Acad. Sci. U. S. A. 113 (2016) 3036–3041.
[27] J.M. Enserink, A.E. Christensen, J. de Rooij, M. van Triest, F. Schwede, H.G. Genieser, S.O. Døskeland, J.L. Blank, J.L. Bos, A novel Epac-specific cAMP analogue demonstrates independent regulation of Rap1 and ERK, Nat. Cell Biol. 4 (2002) 901–906.
[28] H. Poppe, S.D. Rybalkin, H. Rehmann, T.R. Hinds, X.B. Tang, A.E. Christensen, F. Schwede, H.G. Genieser, J.L. Bos, S.O. Doskeland, J.A. Beavo, E. Butt, Cyclic nucleotide analogs as probes of signaling pathways, Nat. Methods 5 (2008) 277–278.
[29] H. Rehmann, Epac-inhibitors: facts and artefacts, Sci. Rep. 3 (2013) 3032.
[30] N.V. Bogatcheva, M.A. Zemskova, Y. Kovalenkov, C. Poirier, A.D. Verin, Molecular mechanisms mediating protective effect of cAMP on lipopolysaccharide (LPS)-induced human lung microvascular endothelial cells (HLMVEC) hyperpermeability, J. Cell. Physiol. 221 (2009) 750–759.
[31] A.A. Birukova, T. Zagranichnaya, E. Alekseeva, G.M. Bokoch, K.G. Birukov, Epac/Rap and PKA are novel mechanisms of ANP-induced Rac-mediated pulmonary endothelial barrier protection, J. Cell. Physiol. 215 (2008) 715–724.
[32] A.A. Birukova, T. Zagranichnaya, P. Fu, E. Alekseeva, W. Chen, J.R. Jacobson, K.G. Birukov, Prostaglandins PGE(2) and PGI(2) promote endothelial barrier enhancement via PKA- and Epac1/Rap1-dependent Rac activation, Exp. Cell Res. 313 (2007) 2504–2520.
[33] X. Cullere, S.K. Shaw, L. Andersson, J. Hirahashi, F.W. Luscinskas, T.N. Mayadas, Regulation of vascular endothelial barrier function by Epac, a cAMP-activated exchange factor for Rap GTPase, Blood 105 (2005) 1950–1955.
[34] R.H. Adamson, J.C. Ly, R.K. Sarai, J.F. Lenz, A. Altangerel, D. Drenckhahn, F.E. Curry, Epac/Rap1 pathway regulates microvascular hyperpermeability induced by PAF in rat mesentery, Am. J. Physiol. Heart Circ. Physiol. 294 (2008) H1188–H1196.
[35] A.A. Birukova, K.G. Birukov, D. Adyshev, P. Usatyuk, V. Natarajan, J.G. Garcia, A.D. Verin, Involvement of microtubules and Rho pathway in TGF-beta1-induced lung vascular barrier dysfunction, J. Cell. Physiol. 204 (2005) 934–947.
[36] A.A. Birukova, I. Malyukova, V. Poroyko, K.G. Birukov, Paxillin-beta-catenin interactions are involved in Rac/Cdc42-mediated endothelial barrier-protective response to oxidized phospholipids, Am. J. Physiol. Lung Cell. Mol. Physiol. 293 (2007) L199–L211.
[37] J. Ng, T. Nardine, M. Harms, J. Tzu, A. Goldstein, Y. Sun, G. Dietzl, B.J. Dickson, L. Luo, Rac GTPases control axon growth, guidance and branching, Nature 416 (2002) 442–447.
[38] H.Y. Yao, L. Chen, C. Xu, J. Wang, J. Chen, Q.M. Xie, X. Wu, X.F. Yan, Inhibition of Rac activity alleviates lipopolysaccharide-induced acute pulmonary injury in mice, Biochim. Biophys. Acta 1810 (2011) 666–674.
[39] N. Schlegel, J. Waschke, cAMP with other signaling cues converges on Rac1 to

stabilize the endothelial barrier- a signaling pathway compromised in inflammation, Cell Tissue Res. 355 (2014) 587–596.

[40] M. Aslam, C. Tanislav, C. Troidl, R. Schulz, C. Hamm, D. Gündüz, cAMP controls the restoration of endothelial barrier function after thrombin-induced hyperpermeability via Rac1 activation, Physiol. Rep. 2 (2014).

[41] R.T. Huang, D. Wu, A. Meliton, M.J. Oh, M. Krause, J.A. Lloyd, R. Nigdelioglu, R.B. Hamanaka, M.K. Jain, A. Birukova, J.P. Kress, K.G. Birukov, G.M. Mutlu, Y. Fang, Experimental lung injury reduces Kruppel-like factor 2 to increase endothelial permeability via regulation of RAPGEF3-Rac1 signaling, Am. J. Respir. Crit. Care Med. 195 (2017) 639–651.